Alpha-1 Antitrypsin Limits Neutrophil Extracellular Trap Disruption of Airway Epithelial Barrier Function

Hudock KM[1,2,3], Collins MS[1], Imbrogno M[1], Kramer EL[3,4], Brewington JJ[3,4], Ziady A[3,5], Zhang N[3,6], Snowball J[2], Xu Y[2,3,7], Carey BC[3,8], Horio Y[2,9], O'Grady SM[10,11], Kopras EJ[1], Meeker J[4], Morgan H[4], Ostmann AJ[4], Skala E[5], Siefert M[5], Gollomp K[12,13], Mangalmurti N[14,15], Trapnell BC[1,3,8] and Clancy JP[16]

[1]Division of Pulmonary, Critical Care & Sleep Medicine, Department of Medicine, University of Cincinnati College of Medicine, Cincinnati, OH; [2]Division of Pulmonary Biology, Cincinnati Children's Hospital Medical Center, Cincinnati, OH; [3]Department of Pediatrics, University of Cincinnati College of Medicine, Cincinnati, OH; [4]Division of Pediatric Pulmonary Medicine, Cincinnati Children's Hospital Medical Center, Cincinnati, OH; [5]Division of Bone Marrow Transplantation and Immune Deficiency, Cincinnati Children's Hospital Medical Center, Cincinnati, OH; [6]Division of Biostatistics & Epidemiology, Cincinnati Children's Hospital Medical Center, Cincinnati, OH; [7]Divisions of Biomedical Informatics, Perinatal Institute, Cincinnati Children's Hospital Medical Center, Cincinnati, Ohio; [8]Translational Pulmonary Science Center, Cincinnati Children's Hospital Medical Center, Cincinnati, OH; [9]Department of Respiratory Medicine, Graduate School of Medical Sciences, Kumamoto University, Kumamoto-shi, Kumamoto, Japan; [10]Departments of Animal Science, University of Minnesota, St. Paul, MN; [11]Department of Integrative Biology and Physiology, University of Minnesota, St. Paul, MN; [12]Division of Hematology, Children's Hospital of Philadelphia, Philadelphia, PA; [13]Department of Pediatrics, University of Pennsylvania Perelman School of Medicine, Philadelphia, PA; [14]Division of Pulmonary, Allergy, and Critical Care Medicine, University of Pennsylvania Perelman School of Medicine, Philadelphia, PA; [15]Pennsylvania Lung Biology Institute, University of Pennsylvania Perelman School of Medicine, Philadelphia, PA; [16]Cystic Fibrosis Foundation, Bethesda, MD

Author to whom correspondence should be addressed – Kristin Hudock, hudockkn@ucmail.uc.edu, phone (513) 803-7819 Office: R4087B, CCHMC

Key Words: NETs, E-cadherin, Alpha-1 antitrypsin, barrier function, bronchial epithelia

---

Abstract

Neutrophil extracellular traps (NETs) contribute to lung injury in cystic fibrosis and asthma, but the mechanisms are poorly understood. We sought to understand the impact of NETs on barrier function in human airway epithelia. To test this, we exposed primary human bronchial epithelial cells (HBE) and a human airway epithelial cell line (wtCFBE41o-) to isolated human NETs in their apical compartment for 2-18 hours. We demonstrate that NETs disrupt airway epithelial barrier function by decreasing transepithelial electrical resistance (TEER) and increasing paracellular flux. This is in part due to NET-induced airway epithelial cell death via apoptosis. NETs selectively impact the expression of the tight junction genes claudins 4, 8 and 11. Intact epithelia exposed to NETs demonstrate visible gaps in E-cadherin staining, a decrease in full-length E-cadherin protein and the appearance of cleaved E-cadherin peptides. DNase did not alter NET-driven changes in HBE TEER or E-cadherin. Pretreatment of NETs with alpha-1 antitrypsin (A1AT) inhibits NET serine protease activity, limits E-cadherin cleavage, and preserves epithelial integrity. In conclusion, NETs disrupt human airway epithelial barrier function through bronchial cell death and degradation of E-cadherin, the latter of which limited by exogenous A1AT.

Graphical Abstract

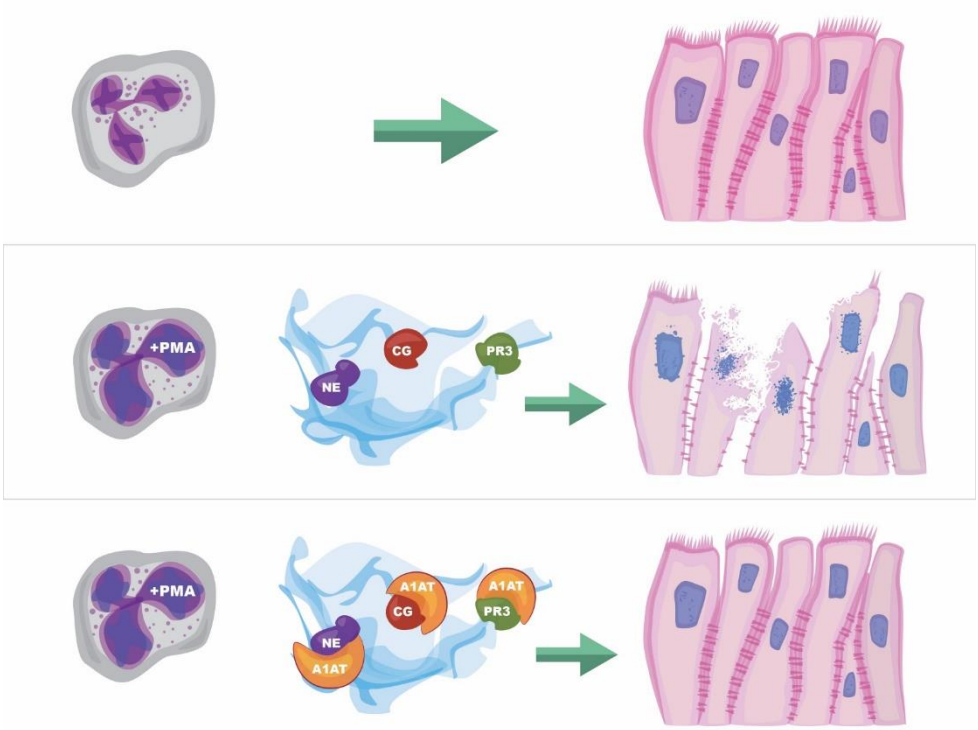

Introduction

Neutrophils play a critical role in innate host defense. Neutrophil extracellular traps (NETs) are web-like structures released by neutrophils in response to numerous pathogens, inflammatory cytokines and other compounds (1-4). NETs trap bacteria in the bloodstream and tissues to limit dissemination to other organs (5-7). NETs also play a role in thrombus formation via multiple mechanisms (8-10). NETs are comprised of a DNA backbone studded with histones, proteases, cytokines and other immunomodulatory molecules (11). The most commonly reported NET proteases are neutrophil elastase (NE) and cathepsin G (CG) (12). NET proteases are enzymatically active even when exposed to recombinant human DNase (13). NET proteases perform functions such as processing of cytokines into active forms (14). NETs have been implicated in perpetuating airway inflammation in conditions including asthma and CF and we have previously reported that NETs can increase IL-8 via activation of the IL-1 pathway (13,15,16). The impact of NETs on other critical epithelial roles such as barrier function, however, remains largely unstudied.

Bronchial epithelia serve an important barrier function to limit entry of pathogens and injurious agents into the submucosa and bloodstream. Human bronchial airways are predominately lined with ciliated pseudostratified columnar epithelial cells and an overlying thin layer of mucus (17). Epithelial cells form an effective barrier through a complex junctional protein network that maintains cell-cell contact and limits paracellular passage (18). Junctional protein structures include tight junctions, adherens junctions, and desmosomes. E-cadherin is a crucial adherens junctional protein that is widely expressed in human epithelia and is a key component of the intact human airway mucosa (19). Respiratory infections, e.g., adenovirus and *Pseudomonas aeruginosa*, are associated with loss of E-cadherin (20,21). Decreased E-cadherin compromising epithelial barrier function has been reported in airway diseases including asthma (19).

Alpha-1 antitrypsin (A1AT) is a naturally occurring serine protease inhibitor that binds to and mitigates the activity of serine proteases including NE, CG and proteinase 3 (PR3). A1AT is predominately

generated by hepatocytes, but production of A1AT by human bronchial epithelia and neutrophils has been described (22-24). A1AT deficiency is due to a protease-antiprotease imbalance that results in unhindered protease activity, increased inflammation and destruction of lung tissue (25). Although A1AT inhibits neutrophil proteases, it is unclear if they effectively bind NET proteases and limit lung epithelial injury.

In the current report we hypothesized that NETs were sufficient to alter airway epithelial barrier function. To test this hypothesis, we exposed primary human bronchial epithelia (HBE) grown at air liquid interface (ALI) and a polarized human bronchial epithelial cell line (wtCFBE41o-) to isolated human NETs *in vitro*. Our work demonstrated that NETs disrupted human airway epithelia barrier function assessed by electrical resistance, transepithelial macromolecule flux, confocal microscopy, and junctional RNA and protein expression. Several NET-driven mechanisms contributed to loss of barrier function, including induction of apoptosis and degradation of E-cadherin. A1AT partially limited NET-driven cleavage of E-cadherin and maintained monolayer resistance. Together, our results demonstrate that NETs produce airway cell injury and death leading to disruption of bronchial epithelial integrity.

Results

Human NETs disrupt epithelial monolayer integrity

We sought to determine if isolated human NETs disrupt barrier function of HBE *in vitro*. Neutrophils were harvested from the peripheral blood of healthy human donors using negative bead selection and exposed to phorbol 12-myristate 13-acetate (PMA) to stimulate NETosis (13,26). As previously described, the resulting viscous layer of NETs was collected and centrifuged to remove cellular debris (26). Primary HBE grown at ALI or wtCFBE41o- cell line expressing wild type CFTR were exposed to isolated NETs in the apical compartment of cell culture inserts. Transepithelial electrical resistance (TEER) was measured to assess the barrier function of the epithelial monolayer at baseline and after exposure to NETs. Both wtCFBE41o- and HBE maintain tight cell-cell junctions across the monolayer reflected by high baseline resistance measurements (686Ω/cm^2 +/- 61.12, 1238Ω/cm^2 +/- 31.62, respectively) (27,28).

wtCFBE41o- cells exposed to NETs for 18 hours had a ~50% decrease in electrical resistance when compared to media control, which was unchanged (Figure 1A). Primary HBE exposed to NETs had a similar average reduction (Figure 1B). Pretreatment of NETs with dornase alpha (DA), a

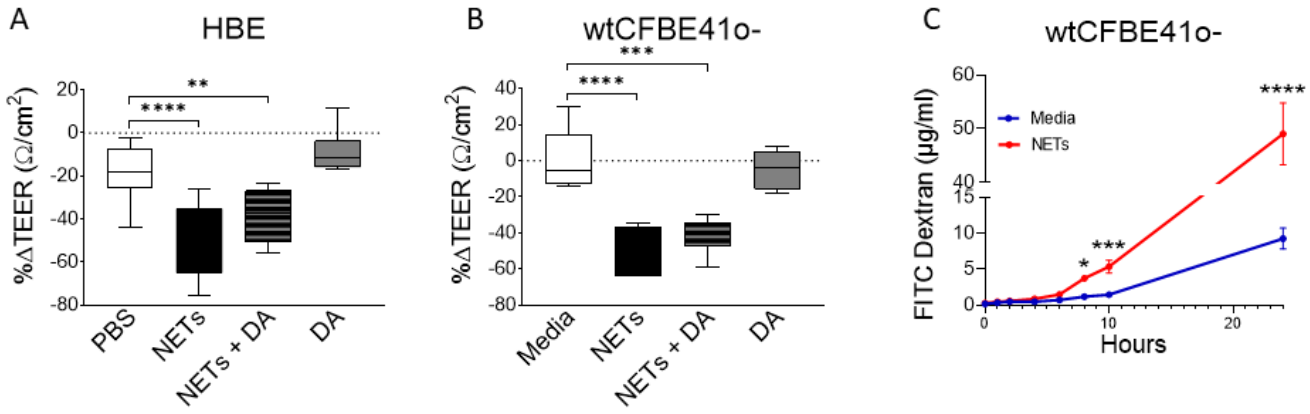

Figure 1. Neutrophil extracellular traps (NETs) disrupt epithelial barrier function.
(A) wtCFBE41o- grown to confluence and **(B)** primary normal human bronchial epithelia (HBE) grown at air-liquid interface (ALI) were exposed to media or PBS control (respectively), 5µg/ml NETs, NETs + 0.5µg/ml dornase alpha (DA), or DA in the apical compartment for 18 hours in triplicate wells. Transepithelial electrical resistance (TEER) was measured pre and post treatment in duplicate for each well and expressed as a percent change. Data analyzed by one-way ANOVA followed by Bonferroni's multiple comparisons test (experiments were performed in triplicate, HBE donors=3, NET donors=4). **(C)** Apical to basolateral flux of FITC labeled dextran across wtCFBE41o- exposed to media control or NETs from 0-24 hours. Data analyzed by Least Squares Means, F-test=264.58, ****p<0.0001 from 8-24 hours (experiments were performed in duplicate, NET donors=2). *p<0.05, **p<0.01, ***p<0.001, ****p<0.0001

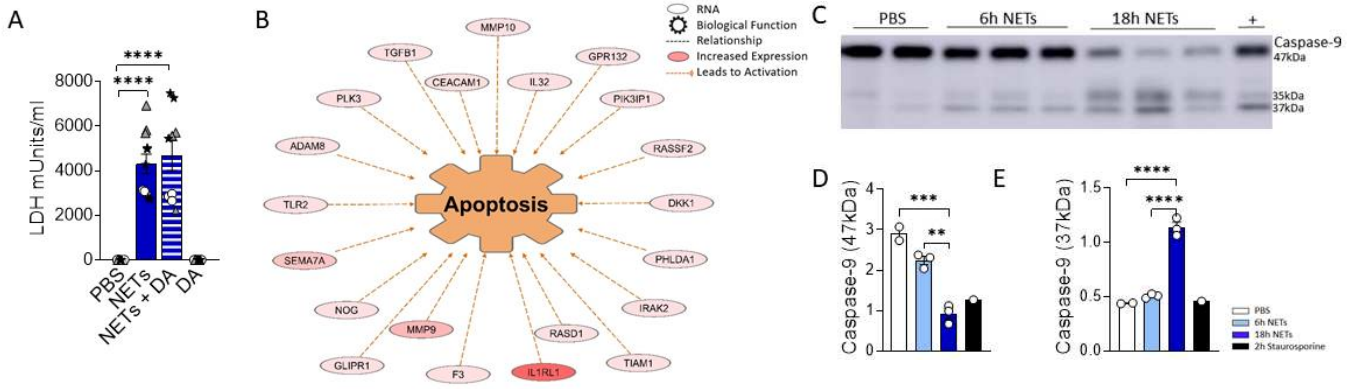

Figure 2. NETs activate apoptosis in normal human bronchial epithelia. HBE were grown at ALI and exposed to PBS control, 5μg/ml NETs, NETs+0.5μg/ml dornase alpha (DA), or DA in the apical compartment 18h in triplicate wells. **(A)** LDH concentration was measured in apical supernatant. Data analyzed by one-way ANOVA followed by Bonferroni's multiple comparisons test (experiments=2, HBE donors=2, NET donors=2). **(B)** Differential gene expression assessed by RNA sequencing in HBE after exposure to 5μg/ml NETs compared to PBS. Network representation of impacted genes predicted to activate apoptosis. Color intensity indicates increased expression. Data analyzed using Ingenuity Pathway Analysis (IPA) (p=1.07e-13, experiments=3, HBE donors=3, NET donors=3). **(C)** Representative western blot of HBE lysates and analyses demonstrate **(D)** decreased full-length caspase-9, **(E)** increased cleaved caspase-9 at 37kDa, indicating apoptosis occurs in HBE exposed to NETs at 6h and 18h compared to PBS. Positive control (+) 16HBE cells treated with staurosporine (5μM, 2h). Data analyzed by one-way ANOVA followed by Bonferroni's multiple comparisons test (experiments=2, HBE donors=2, NET donors=3). **p<0.01, ***p<0.001, ****p<0.0001

DNase therapy prescribed for CF, did not limit NET-driven reductions in resistance (29). DA alone yielded similar results to controls in both HBE and wtCFBE41o-. Resistance measured in primary HBE after 2 and 6 hour NET exposure were unchanged compared to PBS, but significantly decreased at 18 hours (p<0.0001) (Supplemental Figure 1).

To determine if the NET-driven reduction in electrical resistance was associated with altered permeability of the epithelia to large molecules, we monitored the impact of NET exposure on the apical-to-basolateral flux of FITC-labeled dextran across wtCFBE41o- monolayers (30). FITC-dextran concentrations increased significantly in the basolateral media beginning at 8 hours by 68.5% (media control = 0.9-1.4μg/ml vs NETs = 3.4-3.9μg/ml, p=0.0044) through 24 hours by 81.2% (media control = 7.2-11.6μg/ml vs NETs = 41.4-53.0μg/ml, p<0.0001) in wtCFBE41o- cells exposed to NETs (Figure 1C). There was no significant change in FITC dextran flux from 0-6 hours of NET exposure, which is consistent with the lack of change in HBE TEER from 0-6 hours (Supplemental Figure 1). Together, our findings suggest that NET disruption of epithelial monolayer barrier function occurs over time, enhancing paracellular passage of macromolecules.

NETs cause human airway cell death via apoptosis

To determine if changes in epithelial monolayer barrier function were due to NET-induced airway cell injury, we measured lactate dehydrogenase (LDH), an indicator of cytotoxicity (31). LDH increased in the apical supernatant of HBE in response to NET exposure after 18 hours (Figure 2A). LDH release from HBE exposed to NETs or NETs pretreated with DA were similar. DA alone did not cause cytotoxicity to HBE cells. To test if individual components of NETs recapitulated NET-induced cytotoxicity, wtCFBE41o- were exposed to human core histones, genomic DNA , or proteases. Single NET components did not lead to significant LDH release compared with epithelia exposed to intact NETs (Supplemental Figure 2A).

To establish which cell death pathway is triggered by NETs in human airway epithelia, we performed RNA seq on HBE from three donors exposed to NETs from 3 different individuals. A network of fifty-two RNAs involved in apoptosis had significantly increased expression and thirty RNAs had significantly decreased expression (Figure 2B, Supplemental Table 1). CAV1, which was downregulated 5-fold, encodes cavelolin, a scaffolding protein found in plasma membranes which inhibits apoptosis (32). PHLDA1 was increased 6-fold and is known to promote apoptosis via Fas expression (33). RNAs for the interleukin-1 receptor and other pro-inflammatory cytokines were highly upregulated and may contribute to cytokine-driven apoptosis (34,35). We also examined necroptosis, a pro-inflammatory cell death pathway that could contribute to the NET-induced inflammation we previously reported in bronchial epithelia (13,36). NETs had no impact on the expression of genes controlling necroptosis in epithelia after 18 hours of exposure.

To further assess the role of apoptosis in HBE exposed to NETs, cell lysates were analyzed by western blot for activation of caspase-9, an initiator of the intrinsic pathway of apoptosis. Mitochondrial release of cytochrome c, and subsequent apoptotic protease-activating factor-1 (APAF1) activation, cleaves the 47kDa procaspase-9 into active dimers detectable at 35kDa and 37kDa (37). After 6 hours of NET exposure in HBE, there was a trend towards decreasing procaspase-9 and increased cleaved caspase-9 peptides. After 18 hours procaspase-9 was significantly decreased (p=0.0005) and the cleaved caspase 9 peptides significantly increased (p<0.0001) compared to PBS (Figure 2C-E). There was no change in the necroptosis pathway proteins RIP-1, MLKL, or corresponding phosphorylated isoforms in HBE exposed to NETs (Supplemental Figure 2B-C) (38). Together, these data support the observation that NETs activate apoptosis in primary airway epithelia.

NETs damage epithelial cell junctions

We next investigated if NETs disrupt the airway epithelial barrier by impacting cell junctions. RNA sequencing of HBE exposed to NETs identified significant changes in expression of RNAs regulating cell junction organization (Figure 3A-3B and Supplemental Table 2). TIAM1, upregulated 9.7-fold, regulates RAC-1 signaling pathways affecting cell migration, polarity, and cytoskeleton (39). LAMC2, upregulated 8.4-fold, encodes an epithelial protein, which connects cells to the basement membrane (40). SNAI2, downregulated 4.7-fold, is thought to repress E-cadherin transcription (41). Along with upregulation of metalloproteinase genes (Figure 4), involved in extracellular matrix degradation, these transcriptional changes signal the breakdown of cell monolayer architecture (42).

Located in cell-cell tight junctions, claudins are tetraspan transmembrane proteins that regulate paracellular diffusion of ions, anions, and solutes (43). Due to their importance in epithelial barrier function, we chose to focus on our RNA sequencing findings of changes in claudin gene expression. Claudin-4, a tight junction sealing protein and controller of anion flux, significantly increased with NET exposure after 18 hours (44). In contrast, claudin-8 and claudin-11 were significantly downregulated by NETs at 18 hours (Figure 3C). Previously in the kidney, claudin-4 was shown to require claudin-8 for tight junction localization, where it forms an anion channel (45). Claudin-11 is expressed in renal, gastrointestinal and reproductive epithelia, and in the stria of the inner ear (46). Moreover, in Sertoli cells, claudin-11 localization within tight junction strands contributes to the formation of the blood-testis barrier (47). Disruption of barrier function and increased flux caused by NET exposure (Figure 1) is a key finding of our work. These results indicate NETs have selective and specific effects on junctional proteins in HBE.

To visualize the impact of NETs on specific bronchial epithelia junctional proteins, we performed confocal microscopy on wtCFBE41o- and HBE cells exposed to NETs for 18 hours, focusing on staining patterns of the critical and well-

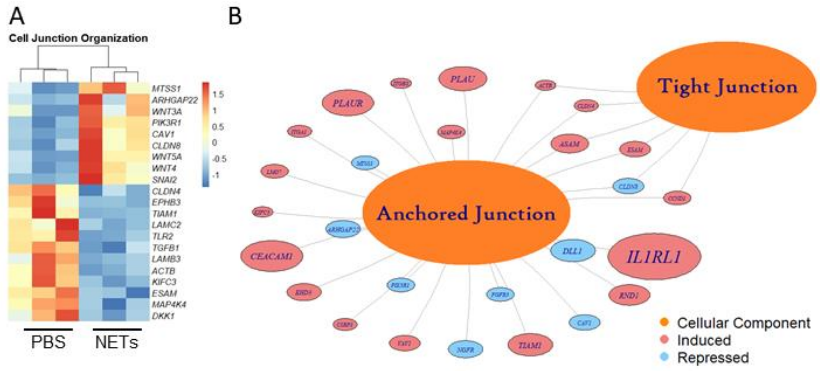

C

	2h		18h		2h vs 18h
Gene	Fold change/PBS	p-value	Fold change/PBS	p-value	p-value
CLDN4	1.96	NS	2.65	<0.0001	NS
CLDN8	0.85	NS	0.17	<0.0001	0.0013
CLDN11	1.74	NS	0.16	<0.0001	0.0004

Figure 3. NETs alter epithelial cell junction genes. HBE grown at ALI exposed to PBS control or 5µg/ml NETs in the apical compartment in triplicate wells. **(A)** Differentially expressed genes involved in cell junction organization were visualized in a z-scored normalized heat map of fragments per kilobase of transcript per million mapped reads (FPKM) demonstrate significant changes in HBE exposed to NETs for 18 hours. **(B)** Functionally enriched RNAs for cellular components of "anchored junctions" and "tight junctions" in HBE impacted by NET exposure for 18 hours, analyzed using ToppGene (experiments were performed in triplicate HBE donors=3, NET donors=3). **(C)** Changes in junctional RNAs after 2 or 18 hour exposure to NETs were confirmed by RT-PCR and normalized to 18S. Data analyzed by unpaired t-test (experiments were performed in triplicate, HBE donors=4, NET donors=3).

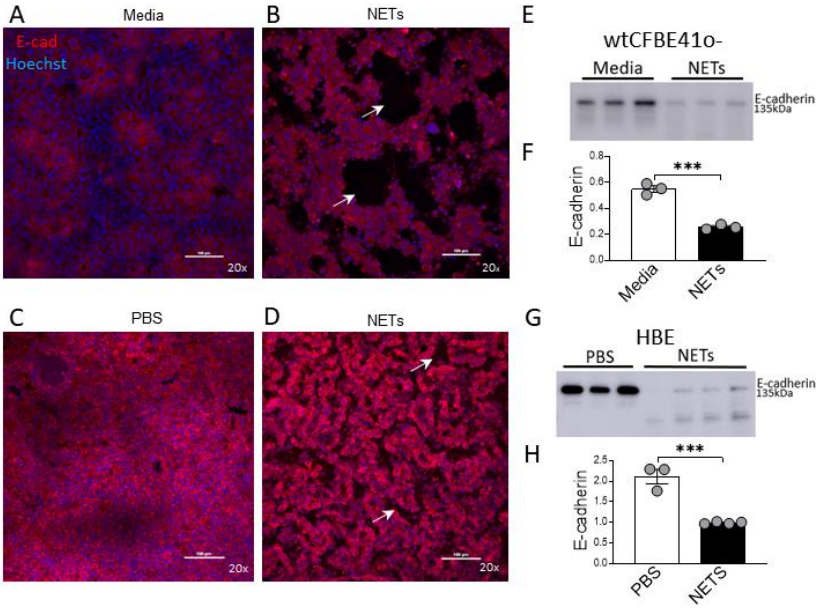

Figure 4. NETs disrupt epithelia and decrease E-cadherin. Confocal microscopy images (20x) of human epithelia stained for E-cadherin/AF647 and DNA/Hoechst. **(A)** wtCFBE41o- grown to confluence exposed to media or **(B)** 16μg/ml NETs for 18h, the latter with visible holes (arrows) in the monolayer. **(C)** HBE grown at ALI exposed to PBS or **(D)** 5μg/ml NETs for 18h, the latter with disruptions (arrows) in the monolayer. **(E)** Representative western blot and **(F)** corresponding analysis of E-cadherin protein from wtCFBE41o- lysates after 18h incubation with PBS or 16μg/ml NETs. E-cadherin normalized to C4-actin. Data analyzed by unpaired t-test (***p=0.0004, experiments performed in duplicate, NET donors=2). **(G)** Representative western blot and **(H)** analysis of E-cadherin protein from HBE lysates after 18h incubation with PBS or 5μg/ml NETs. E-cadherin normalized to C4-actin. Data analyzed by unpaired t-test (experiments were performed in triplicate, HBE donors=3, NET donors=3). ***p<0.001

characterized E-cadherin protein (Figure 4). High-dose NET exposure led to the formation of gaps in the previously confluent wtCFBE41o- monolayer (Figure 4A-B). Images revealed partial loss of E-cadherin mediated cell-cell attachments in HBE monolayers exposed to NETs (Figure 4C-D). Western blotting demonstrated significant reductions of E-cadherin protein in wtCFBE41o- (Figure 4E-F) and in HBE (Figure 4G-H) in response to NETs compared with control. Pretreatment of NETs with DA had no effect on loss of E-cadherin at 18 hours in wtCFBE41o- cells (Supplemental Figure 3A-B). NET-driven decreases in HBE E-cadherin were time-dependent with a trend toward reduction at 6 hours and a significant decrease in E-cadherin protein of 66.9% (p=0.0052) at 18 hours (Supplemental Figure 3C-D).

Alpha-1 antitrypsin limits NET-driven E-cadherin degradation

NETs are rich with serine protease enzymes, which exert antimicrobial effects (48). Given the complex structure of NETs and their associated proteases, we tested the susceptibility of NET proteases to inhibitors. Protease inhibitors decreased NET protease activity in a concentration-dependent manner in the absence of epithelial cells (Supplemental Figure 4A-C). NETs from three donors were separately exposed to A1AT, CG inhibitor (CGI), NE inhibitor sivelestat (SIV), pan-protease inhibitor III (PPI), or heat-inactivated NETs (HIN) for one hour. Heat reduced the activity of CG, PR3, and NE in NETs by 90-100%. A1AT reduced all three NET serine protease activities. CGI was a potent and specific inhibitor of CG, while SIV was most effective against NE and PR3. PPI was a less effective inhibitor overall. Reductions in activity differed across NET donors, suggesting varying susceptibility to protease inhibition. We also tested the effect of A1AT and NETs in the apical supernatant of HBE, where endogenous molecules may alter activity or compete for binding. A1AT was an effective NET serine protease inhibitor in the presence of HBE, significantly decreasing NE, CG, and PR3 activity (p<0.0001) in apical supernatants at 18 hours (Figure 5A-C).

To test the role of NET proteases in the degradation of E-cadherin, we exposed HBE to NETs with and without A1AT pretreatment. NETs caused cleavage of E-cadherin into 68, 72, and 77kDa fragments not observed in HBE exposed to PBS or A1AT alone (Figure 5D-E). A1AT pretreatment of NETs significantly maintained full-length E-cadherin (135kDa) in HBE exposed to NETs (Figure 5D). Next, we sought to determine if A1AT stabilized the electrical resistance of epithelial monolayers exposed to NETs. Importantly, pretreatment of NETs with A1AT preserved resistance compared to HBE exposed to NETs (Figure 5F).

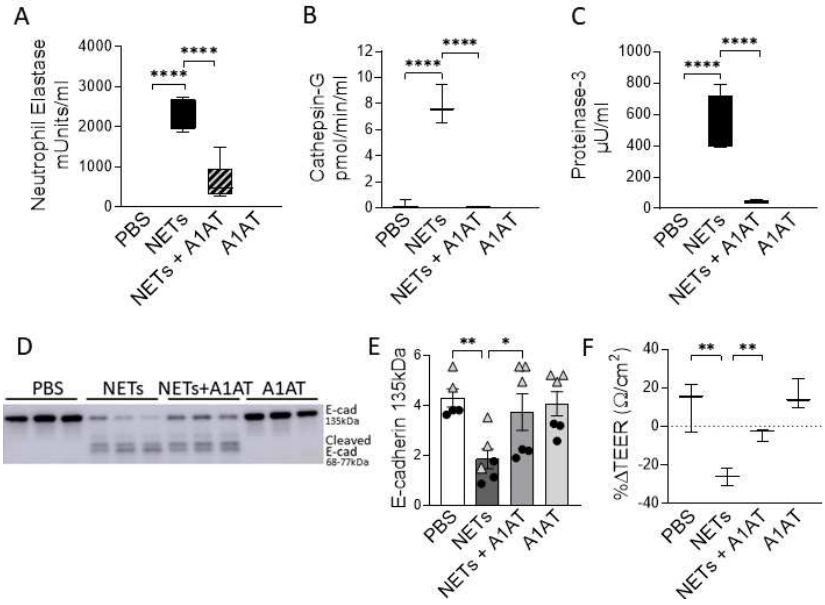

Figure 5. Alpha-1 antitrypsin reduces NET-driven degradation of E-cadherin. HBE were exposed to PBS, 5µg/ml NETs, NETs+100µg/ml A1AT or A1AT for 18h in triplicate wells. **(A-C)** Activity of NE, CG, and PR3 were reduced in the apical supernatants of HBE exposed to NETs + A1AT. Data analyzed by one-way ANOVA followed by Bonferroni's multiple comparisons test (experiments=3, HBE donors=4, NET donor=2). (**D-E)** Representative western blot and analysis of E-cadherin protein from HBE lysates demonstrate that NET exposure significantly decreases (p=0.0016) the concentration of full-length E-cadherin (135kDa) and increases (p=<0.0001) cleaved E-cadherin (68 and 72kDa) compared to PBS control. A1AT significantly *limits* (p=0.0487) NET-driven reductions in full-length E-cadherin protein. Western blots normalized to C4-actin and analyzed by one-way ANOVA followed by Bonferroni's multiple comparisons test (experiments=2, HBE donors=2, NET donors=3). **(F)** HBE exposed to NETs + A1AT had higher TEER than HBE exposed to NETs alone (representative graph). Data analyzed by unpaired t-test (experiments=3, HBE donors=3, NETs=3). *p<0.05, **p<0.01,

A1AT complexes with NET neutrophil elastase

While A1AT binds and inactivates serine proteases from neutrophils, it is unclear whether A1AT binds NET proteases directly (49). To demonstrate direct binding of A1AT to NET NE, we performed western blots on supernatants of HBE exposed to NETs with and without A1AT pretreatment. In blots probed for A1AT, 51 and 55kDa A1AT bands and an 80kDa A1AT:NE co-localizing band were detected (Figure 6A). A1AT alone was not detected by western blot in the supernatants of HBE exposed to NETs (Figure 6A). In blots probed for NE, a 29kDa NE band and the A1AT:NE complex were detected (Figure 6B). Most of the NE in NETs pretreated with A1AT co-localized with A1AT (Figure 6B). To further demonstrate NE:A1AT binding, we performed co-immunoprecipitation and detected the NE:A1AT complex (Supplemental Figure 4D).

To confirm our findings that NET NE complexes with A1AT we analyzed supernatants of HBE exposed to NETs with and without A1AT by mass spectrometry (Figure 6C). There were peptide spectral matches (PSMs) for CG, PR3, and NE detected at 17-31kD. There was a low level of full length A1AT detected, potentially from NETs or secreted by HBEs. There was no detectable A1AT:NE complex in the absence of exogenous A1AT. There were PSMs for CG, PR3, NE and A1AT at 70-102kDa in HBE supernatants exposed to NETs pretreated with A1AT, which represent the individual proteases complexing with A1AT. Also in the HBE supernatant exposed to NET pretreated with A1AT were peptide fragments of A1AT at 17-31kDa, likely the result of partial cleavage by other NET proteases. These mass spectrometric findings support the notion that A1AT directly forms complexes with NET proteases and limits NET-induced degradation of E-cadherin and disruptions in epithelial barrier function.

Discussion

NETs are associated with lung injury in many diseases, but the mechanisms of injury remain unclear (50,51). Our results demonstrate that NETs were sufficient to reduce electrical resistance in human airway cells and produced an increase in the paracellular flux of macromolecules. NET exposure activated transcription of genes promoting apoptotic cell death, which was confirmed by increased cleavage of the apoptosis initiator caspase-9 protein. In addition to NET-induced cytotoxicity, we observed selective changes in expression of tight junction genes including *CLDN4*, *CLDN8* and *CLDN11* in surviving epithelial cells. Bronchial epithelia exposed to NETs had visible disruptions in E-cadherin staining and reductions in E-cadherin protein in cell lysates. A1AT partially blocked NET-induced E-cadherin degradation and TEER reduction, emphasizing the role of NET serine proteases in epithelial injury. Collectively, these findings support the hypothesis that NETs induce epithelial cell death and regulate the expression of

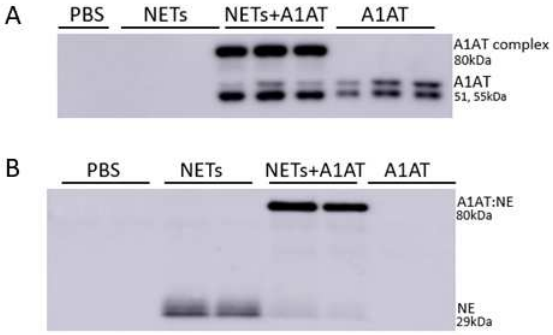

C

	NETs			NETs + A1AT		
	17-31kDa	50-60kDa	70-102kDa	17-31kDa	50-60kDa	70-102kDa
Alpha-1-antitrypsin (A1AT)	23	18		934	1757	1683
Cathepsin G (CG)	125	4		99	11	15.5
Myeloblastin (PR3)	5			9		7
Neutrophil elastase (NE)	188		18	132	18	1026

Figure 6. Alpha-1 antitrypsin binds serine proteases in NET exposed HBE. HBE grown at ALI were exposed to PBS, 5µg/ml NETs, NETs+100µg/ml A1AT or A1AT for 18h in triplicate wells. **(A)** Western blot of HBE apical supernatants probed with anti-A1AT antibody demonstrate the colocalization of A1AT (51-55kDa) with a 29kDa serine protease in NETs. **(B)** Western blot of HBE apical supernatants probed with NE antibody demonstrate the specific colocalization of A1AT with NE (29kDa) in NETs forming an 80kDa complex. **(C)** Mass spec. of bands shown on western blot in A & B confirm that HBE exposed to NETs have PSMs that correspond to CG, PR3, and NE at the expected 17-31kDa size. HBE exposed to NETs in the presence of A1AT demonstrate PSMs corresponding to NE and A1AT at 70-102kDa indicating formation of an A1AT:NE complex (experiments=3, HBE donors=3, NET donors=3).

specific junctional proteins leading to disrupted epithelial barrier integrity (Figure 7).

Elevated airway NET levels and disruption of epithelial barrier function have been observed in asthma and CF, but mechanistic links are needed (15,52-54). Direct cleavage of junctional proteins or changes in expression of junctional molecules, both of which we demonstrate, have been reported to alter barrier function in lung diseases and infections (21,55,56). Evidence for barrier dysfunction in CF comes from glucose gradients in the blood that reflect airway concentrations, changes in claudin-3 expression in CF epithelia, and alterations in paracellular flux across CF epithelia (57,58). Similar findings of barrier function disruption have been reported in asthma, including altered junctional protein expression, which is exacerbated by infection (15). Although beyond the scope of this work, we postulate that changes in junctional RNAs could also be due to indirect effects of NETs on epithelia, e.g., cell stress or NET-induced changes in epithelial cytokines (13,57) Our findings that isolated NETs have multifaceted impacts on epithelial barrier function are, therefore, relevant for many diseases.

Airway epithelia have been described as relatively resistant to apoptosis, which when it occurs, disrupts barrier function (59,60). Multicaspase activation is suggested to be caused by NETs in an alveolar adenocarcinoma cell line, whereas we demonstrate that NETs induce apoptosis in primary human bronchial epithelia (61). Individual NET components did not cause the cytotoxicity produced by intact NETs in airway epithelia despite isolated histones or neutrophil proteases producing cell death in other models (61,62). These findings suggest that NET-induced cell death is likely multifactorial. Many of the pro-apoptotic transcriptional changes observed in our NET-exposed human bronchial epithelia included upregulation of proinflammatory cytokine pathways (13). Although beyond the scope of this current work, NET- induced cytokine changes could be driving the airway epithelial cell apoptosis observed in our models (13,63).

A key finding of our work is that NET exposure selectively cleaves E-cadherin, a junctional protein expressed at the basolateral surface of airway cells and an important regulator of monolayer integrity (64). The importance of E-cadherin in bronchial epithelia barrier function has been shown in the 16HBE41o- cell line in which blockade of E-cadherin decreased electrical resistance of the monolayer and enhanced adenoviral infection (20). E-cadherin has multiple potential cleavage sites for NET serine proteases (protein prospector). Although purified NE, CG, and PR3 have been shown to cleave E-cadherin in bronchial cell lines *in vitro*, to our knowledge, this is the first demonstration that human NETs cleave E-cadherin resulting in altered barrier function in primary human bronchial epithelia (65,66).

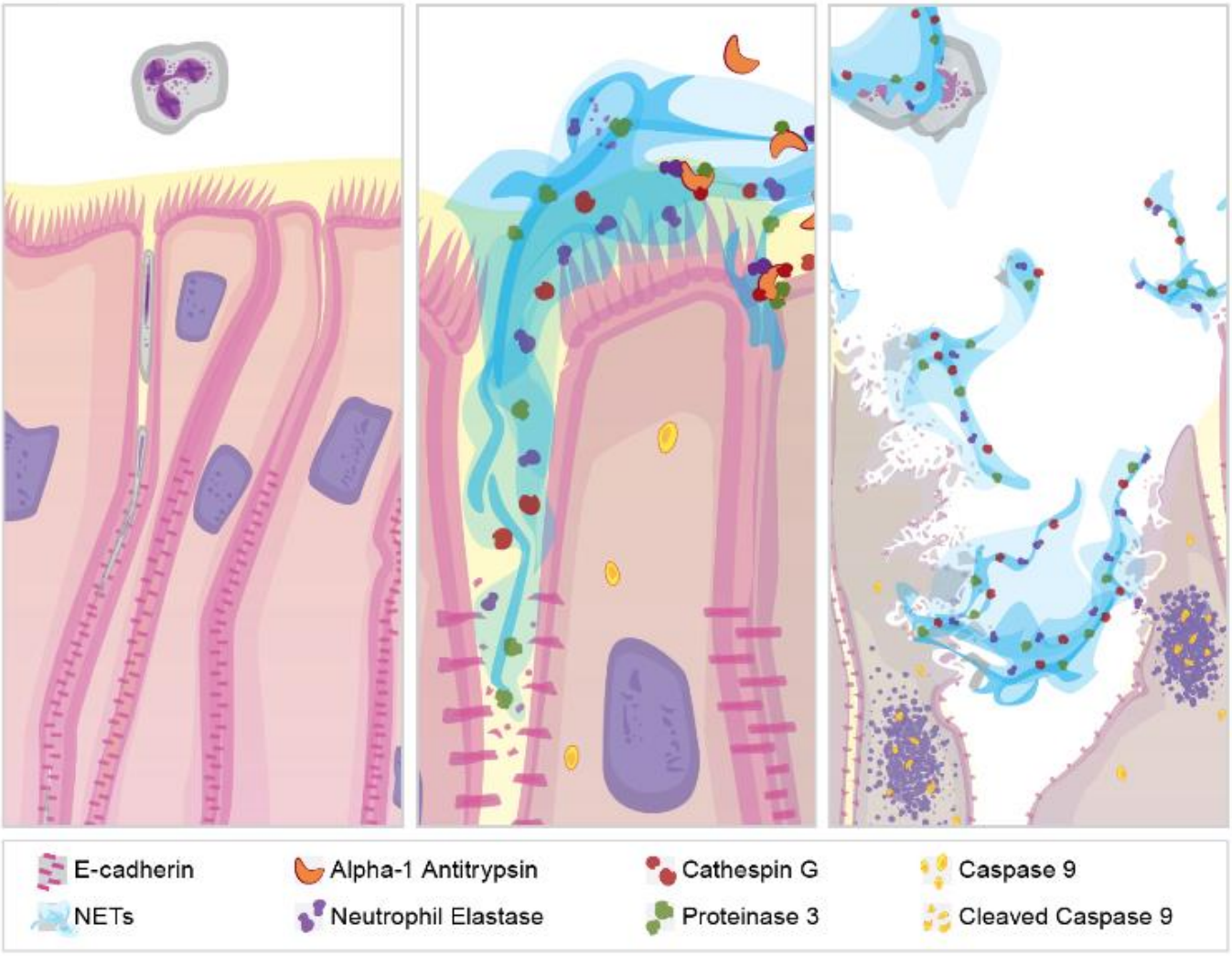

Figure 7. NET effect on airway epithelial barrier function. (A) Pseudostratified bronchial epithelia form a monolayer with cell-cell contact via junctional proteins. This epithelial barrier tightly controls the paracellular flux of molecules and cells. **(B)** Various stimuli cause neutrophils to expel NETs which contain biologically active proteases that degrade adherens junction protein E-cadherin creating gaps in the monolayer. A1AT limits NET degradation of E-cadherin to restore barrier function. C) NETs also disrupt barrier function by causing epithelial cell death via apoptosis.

Protease-antiprotease imbalance has been postulated to contribute to many pulmonary diseases, including COPD and alpha-1 antitrypsin deficiency (67,68). NE levels and activity are elevated in bronchoalveolar lavage fluid (BALF) from infants with CF, even in the absence of infection, and is associated with early bronchiectasis (69,70). Increased neutrophil numbers and NE activity are also associated with severe asthma and bronchodilator resistance (71,72). Whether NET-derived NE (and/or other proteases) contribute to these relationships between NE and airway disease pathology is unknown.

We next examined whether the naturally occurring serine protease inhibitor A1AT was sufficient to impact NET damage to airway epithelia integrity. Colocalization of fluorescently labeled A1AT and NE in NETs, generated *ex vivo* from alpha-1 antitrypsin deficient patients receiving recombinant A1AT therapy, has been reported but the functional implications have not (73). In addition to demonstrating that A1AT binds NET serine proteases, we show that it inhibits NET protease activities. The importance of our finding that NET NE complexes with A1AT is that NE is known to cleave A1AT, which causes a change in A1AT conformation. This produces formation of a covalent bond between NE and A1AT that renders both molecules inactive (74-76). Furthermore, this could lead to NET depletion of endogenous A1AT further suggesting that, A1AT augmentation therapy may be critical to limit destruction of lung tissue in conditions with high NET burden.

Our findings show potential for an anti-protease therapy to disrupt NET effects, offering new

therapeutic directions to ameliorate diseases with a high NET burden. A strength of our study was that we used NETs from six donors and primary airway epithelia from 10 human donors reflecting the broad variability between individual subjects. Previously, others and we have reported variability in the concentration and protease activities of NETs from different human subjects, which contributes to variability in results between groups of investigators (13,77). Additionally, we demonstrated similar epithelial responses to NETs across both primary airway epithelial and a bronchial epithelial cell line reinforcing the validity of our findings and likely relevance to *in vivo* conditions. Notably, our most critical findings of NET cleavage of E-cadherin and disruption of epithelial barrier function with amelioration by A1AT were consistent across NET and epithelial donors. An additional strength is that our demonstration of a cohesive sequence of NET-induced events involving epithelial disruption, apoptosis, and destruction of the monolayer has implications in both acute and chronic lung diseases, e.g., ARDS and CF.

Limitations of our studies include defining NET "dosage" by DNA content alone, which despite acceptance in the field, does not account for 100+ other NET components (12,61). We have attempted to address this limitation by using multiple primary HBE cell and NET donors, but acknowledge this contribution to variability in our results. Our *in vitro* studies demonstrate that NETs can cause epithelial cell cytotoxicity, but whether this occurs *in vivo* is unknown. Our study is not designed to test if NET proteases, surrounded by a complex structure of DNA and histones, are more injurious and less susceptible to inhibitors compared with unbound proteases. Additionally, our experiments do not factor in the positive effects of NETs, which include limiting the spread of pathogens (5,6).

In summary, we present a novel paradigm in which NETs are sufficient to disrupt human airway epithelial barrier function by causing bronchial epithelial apoptosis, altered regulation of junctional protein expression, and cleavage of E-cadherin, the latter of which is limited by exogenous A1AT. NET-driven injury to the airway epithelium is a pathway of inflammatory damage relevant to many airway diseases and further investigations may lead to novel therapeutic strategies to mitigate lung function decline in CF and asthma. Finally, NET-driven decreases in E-cadherin have potential consequences that extend beyond disruption of epithelial barrier function and future studies will delve into this biology.

Methods

Generation of Human NETs

Polymorphonuclear (PMN) cells were isolated from the peripheral blood of healthy adult human subjects via negative bead selection using the MACSxpress Neutrophil Isolation Kit, Human (Miltenyi Biotec), as previously described (13). NETs from six different donors were utilized to capture the biologic variability contributed by individuals' neutrophils and are represented on graphs as distinct symbols. Purified PMNs were stimulated with 25nM phorbol 12-myristate 13-acetate (PMA; Millipore-Sigma) and incubated at 37°C, 5% CO_2 for 4 hours to induce NET generation (41). Following incubation, the viscous surface layer of NETs was washed with PBS for HBE studies, or media for wtCFBE41o- experiments, scraped from the dish, and processed as previously reported to yield cell-free human NETs (13). NET dosage was defined by DNA concentration, as previously described (13,61).

Primary HBE and wild-type CFTR CFBE41o- Cell Culture and Treatment

The CCHMC CF Research Development Program Translational and Model Systems Cores maintained, and provided wild-type CFTR (wtCFBE41o-) cells as previously described (28). wtCFBE41o- cells stably transduced with wild-type CFTR were initially generated and described by Gruenert and colleagues, and were initially a kind gift from the University of Alabama at Birmingham (27). HBE from ten normal healthy donors were obtained from University of North Carolina Airway Cell Core using previously described methods (78). HBE at passages 2-3 were differentiated and grown at ALI on Corning® 3470 Transwell® polyester membrane cell culture inserts, 6.5 mm diameter, 0.4µm pore size, by the CCHMC Pulmonary Core as described (28). The CCHMC, Pulmonary Biorepository Core, and University of Cincinnati IRBs approved primary HBE use. Epithelial cells were incubated with NETs from unrelated human donors, at doses of ~5µg/ml, 18h, 37°C, 5% CO_2. Higher dose NETs or other incubation periods were used in experiments where indicated. Dornase Alpha (DA), obtained from the CCHMC research pharmacy, was used at a final concentration of 0.5µg/ml to digest the NET DNA structure.

Transepithelial Electrical Resistance (TEER)

TEER was measured across each epithelial cell layer in duplicate before and after exposure to NETs, controls, and other reagents using an Epithelial Volt/Ohm Meter and chopstick electrode set (World Precision Instruments) as previously

described (28). Results are expressed as percent change from baseline values.

Collection and Characterization of Cell Supernatants

Cells were exposed on their apical surface to controls, NETs or other test compounds in a final volume of 200µl per 6.5mm insert. Supernatants were collected from the apical surface, and aliquots were stored at -80°C. Assays were performed to measure human NE (Cayman Chemical 600610), CG (Cayman Chemical 14993, ABCAM 126780), PR3 (Cayman Chemical 9002021) (30), LDH (Promega). NETs contain LDH, which was subtracted from the total to determine the contribution by HBE. The NET LDH was measured by incubating NETs alone for 18h at 37°C. Across multiple experiments the mean was 675mU/ml. All assays were performed per manufacturer's instructions. Absorbance and fluorescence quantitation was performed using Molecular Devices FlexStation 3.

Protein Isolation and Western Blot

Epithelial cells were lysed using cOmplete Lysis-M, (Roche Diagnostics) and protein was harvested as described (14). Protein concentrations were measured using DC Protein assay (BioRad) with bovine serum albumin (BSA) (Thermo-Fisher) standards. Proteins were separated and immobilized using NOVEX electrophoresis and transfer apparatus, 4-20% Tris-glycine gels, and 0.45µm PVDF membrane (Thermo-Fisher). Western blot was performed as previously described (79). Protein lysates of 16HBE cells exposed for 2h to 5µM staurosporine, (Thermo-Fisher) were used as a positive control for apoptosis. Antibodies for western blot were obtained from Cell Signaling Technology (CS) and Abcam (AB). We used CASP9 CS9502, E-cadherin CS3195, A1AT AB207303, NE AB68672, RIP1 CS3493, MLKL CS14993, p-MLKL CS91689 and C4 anti-actin (Seven Hills Bioreagents LMAB-C4). Secondary antibodies were rbHRP (CS7074) and msHRP (CS7076). Blots were developed using ECL Prime detection reagent (Amersham). Images and analysis were performed using Amersham Imager 600.

RNA Isolation and Sequence Analysis

RNA sequencing analyses (RNA-seq) was performed on primary HBE data previously generated and described (13). Differentially expressed genes had a fold change >2.5, a p-value (negative binomial Test) <0.01, and reads per kilobase million (RPKMs) >2 for 50% of the samples in at least one condition. Ingenuity Pathway Analyses (IPA) was used to predict activation or repression of known biological process or pathways and was used to visualize predicted "apoptosis" activation (80). Functional Enrichment analyses was done using Toppfun to determine biological functions or cellular components enriched in genes differentially regulated following NETs exposure (81). Significant, relevant biological functions or cellular components were visualized in a z-score normalized Fragments Per Kilobase of transcript per Million mapped reads (FPKM) heatmap using pheatmap (https://cran.r-project.org/web/packages/pheatmap/index.html) or a Kamada-Kawai layout generated network using igraph (https://cran.r-project.org/web/packages/igraph/index.html), respectively. Quantitative PCR was performed with TaqMan master mix and primers CLDN4 (Hs00976831), CLDN8 (Hs 04186769) CLDN11 (Hs00194440) normalized to EUK 18S rRNA AB (1207030) (Millipore-Fisher Scientific).

Immunofluorescence Microscopy

Cell culture monolayers were prepared as previously described (14). Briefly, cells were fixed in 4% paraformaldehyde (Fisher Scientific), washed and incubated with mouse anti-human E-cadherin antibody (Cell Signaling Technologies), Alexafluor AF647 (Cell Signaling Technologies), and Hoechst (Invitrogen). Confocal Images were captured on a Nikon A1R GaAsP inverted SP microscope, and analyzed using IMARIS software.

Mass Spectrometry

Modified proteomic methods previously established by Ziady et.al. were used (82-84). The database included A1AT, CG, PR3 (myeloblastin), and NE. The following conditions were tested: NETs and NETs + A1AT. Proteins from each condition were separated on a 4-20% Criterion™ Tris-HCL gel, and bands of interest were excised from the gel at three molecular weight ranges: 17-31kDa, 50-60kDa, and 70-102kDa. The samples were then subjected to in-gel trypsin digest (Trypsin Gold, Mass Spectrometry Grade. Promega. 20µg/ml). Samples were loaded in an UltiMate 3000 HPLC autosampler system (Thermo Fisher) and were eluted using reverse-phase column chromatography into an LTQ Velos Pro with a nanospray ion source. The mass analyzer used data-dependent settings with dynamic exclusion enabled: repeat count = 2; repeat duration = 10 seconds; exclusion list size = 100; exclusion duration = 10 seconds; exclusion mass width = 1.5 amu. Collision-induced dissociation (CID) was used to fragment peptides, and CID spectra were

searched against a human FASTA database using the Proteome Discoverer™ software version 2.4. We used a 5 score cutoff in addition to a 1.0 XCorr threshold. The protein score is the sum of all peptide XCorrs for that protein above a certain threshold. This threshold is determined by the peptide charge and a set peptide relevance factor of 0.0 – 0.8. Proteins were quantified based on peptide spectral match (PSM). Each protein must have a minimum of 2 peptides.

Immunoprecipitation

Immunoprecipitation of A1AT and NE proteins was carried out using supernatants from HBE incubated with PBS, NETs, 100µg/ml A1AT, and NETs pretreated with A1AT. Protein A Dynabeads (Thermo Fisher) were washed with PBS. Samples were incubated with washed beads 1h, 4°C. Pre-cleared samples were incubated with A1AT or NE antibodies (Abcam 207303, 68672) 1h, 4°C. Washed beads were added and incubated overnight at 4°C with rotation. Beads were washed twice in PBS, and proteins eluted with 1X Laemmli buffer 100°C 10 minutes. Resulting proteins were run on an SDS PAGE gel, transferred to PVDF membrane, and probed with corresponding NE or A1AT antibodies.

Dextran Flux Measurements

wtCFBE41o- monolayers were grown to resistances of >600Ωcm^2 on cell culture inserts. FITC-labeled dextran (molecular mass 4,000Da, Sigma-Aldrich, 2.0mg/ml) in media +/- NETs was added to the apical compartment. At each time point, 100µl samples of the basolateral solutions were removed to opaque 96-well plates. Fluorescence intensity (485nm excitation/530nm emission wavelengths) was measured using Molecular Devices FlexStation 3 plate reader. To determine dextran concentration, a standard curve was generated using FITC-dextran dilutions of 0.61-620µg/ml and unidirectional fluxes at each time point were calculated (30).

Protease Inhibitors and Individual NET Components

NETs were pre-incubated with A1AT protein from human plasma (Cayman Chemical) 1h before exposure to HBE. Individual components of NETs were incubated with wtCFBE41o- to assess the effect of each on cytotoxicity and monolayer integrity. These included 5µg/ml human gDNA (Promega), 50µg/ml human core histones (Sigma), 2U/ml human NE protein (Athens Research & Technology, ART), 500µU/ml human PR3 protein (ART) and 4.5mU/ml human CG protein (ART). These were compared to media control, 5µg/ml NETs and 5µg/ml heat inactivated NETs (60°C 10min.). The concentration of individual NET components was chosen to reflect that found in our isolated human NETs. In epithelial cell-free experiments, NETs were pre-incubated with protease inhibitors: human A1AT protein, sivelestat, and cathepsin G inhibitor (Cayman Chemical) all at 1µg/ml and 100µg/ml, and protease inhibitor cocktail III at 0.1µM and 100µM (Alfa Aesar) (1h at 37°C) and assayed for protease activity (85).

Statistical Analysis

Statistical analyses were performed using GraphPad Prism software v7.04 and SAS v9.4. Groups were compared using one-way ANOVA with Bonferroni's correction for multiple comparisons or a Student's t-test where indicated. Data are expressed as means +/- SEM. A p-value of <0.05 was considered significant. Graphs include data from at least three separate experiments unless indicated. Each experiment included conditions run on triplicate or more wells (as noted in figure legends). As per GraphPad analysis, p values ≥ 0.05 are not significant, p-values <0.05 are denoted by *, p-values ≤ 0.01 are denoted by **, p-values ≤ 0.001 are denoted by ***, and p- values ≤ 0.0001 are denoted by ****. In each figure, the number of experimental repeats with similar results is noted. "NETs =" refers to the number of normal human neutrophil donors from which NETs were isolated. "HBE donors =" refers to donors of primary bronchial epithelia samples obtained from the University of North Carolina Airway Cell Core. A total of 10 HBE donors and 6 NETs donors were used in this study. A linear mixed effect model was used to evaluate whether wtCFBE41o- cells exposed to NETs had significantly different dextran flux over the course of 0-24h, compared to media control alone. If a difference existed, post-hoc comparisons were conducted to compare dextran flux between NETs and media control only group at each time point.

Study Approval

The study protocol, no. 2016-3837, was approved by the University of Cincinnati IRB. Healthy adult human subjects provided written informed consent prior to participation in our study.

Author Contributions

Designing research studies: KMH, MSC, MI; conducting experiments: MSC, MI, ES, MS, JM, HM, AJO; analyzing data: KMH, MSC, MI, ES, AZ, NZ, JS, YX; intellectual content; KMH, MSC, MI, ELK, JJB, AZ, SMO, EK, KG, NM, BCT, JPC;

writing the manuscript: KMH, MSC, MI; revisions: all authors.

Acknowledgements

Graphical abstract and illustrations by Laura Collins, Freiburg, Germany.

Funding

NIH NHLBI 1K08HL124191, CFF K Boost HUDOCK20, NIH NHLBI K08HL124191-04S1, RDP CCHMC, Cystic Fibrosis Foundation, Parker B Francis Fellowship, CFF NAREN19R0, HL148856 and HL153045

Bibliography

1. Young RL, Malcolm KC, Kret JE, et al. Neutrophil extracellular trap (NET)-mediated killing of Pseudomonas aeruginosa: evidence of acquired resistance within the CF airway, independent of CFTR. *PLoS One*. 2011;6(9):e23637.

2. Veras FP, Pontelli MC, Silva CM, et al. SARS-CoV-2-triggered neutrophil extracellular traps mediate COVID-19 pathology. *J Exp Med*. 2020;217(12):e20201129. doi: 10.1084/jem.20201129.

3. Keshari RS, Jyoti A, Kumar S, et al. Neutrophil extracellular traps contain mitochondrial as well as nuclear DNA and exhibit inflammatory potential. *Cytometry A*. 2012;81(3):238-247.

4. Kenny EF, Herzig A, Kruger R, et al. Diverse stimuli engage different neutrophil extracellular trap pathways. *Elife*. 2017;6:10.7554/eLife.24437.

5. McDonald B, Urrutia R, Yipp BG, Jenne CN, Kubes P. Intravascular neutrophil extracellular traps capture bacteria from the bloodstream during sepsis. *Cell Host Microbe*. 2012;12(3):324-333.

6. Thanabalasuriar A, Scott BNV, Peiseler M, et al. Neutrophil Extracellular Traps Confine Pseudomonas aeruginosa Ocular Biofilms and Restrict Brain Invasion. *Cell Host Microbe*. 2019;25(4):526-536.e4.

7. Gollomp K, Sarkar A, Harikumar S, et al. Fc-modified HIT-like monoclonal antibody as a novel treatment for sepsis. *Blood*. 2020;135(10):743-754.

8. Gollomp K, Kim M, Johnston I, et al. Neutrophil accumulation and NET release contribute to thrombosis in HIT. *JCI Insight*. 2018;3(18):e99445. doi: 10.1172/jci.insight.99445. eCollection 2018 Sep 20.

9. Fuchs TA, Brill A, Duerschmied D, et al. Extracellular DNA traps promote thrombosis. *Proc Natl Acad Sci U S A*. 2010;107(36):15880-15885.

10. Shi Y, Gauer JS, Baker SR, Philippou H, Connell SD, Ariëns RAS. Neutrophils can promote clotting via FXI and impact clot structure via neutrophil extracellular traps in a distinctive manner in vitro. *Sci Rep*. 2021;11(1):1718-7.

11. Brinkmann V, Reichard U, Goosmann C, et al. Neutrophil extracellular traps kill bacteria. *Science*. 2004;303(5663):1532-1535.

12. Chapman EA, Lyon M, Simpson D, et al. Caught in a Trap? Proteomic Analysis of Neutrophil Extracellular Traps in Rheumatoid Arthritis and Systemic Lupus Erythematosus. *Front Immunol*. 2019;10:423.

13. Hudock KM, Collins MS, Imbrogno M, et al. Neutrophil extracellular traps activate IL-8 and IL-1 expression in human bronchial epithelia. *Am J Physiol Lung Cell Mol Physiol*. 2020;319(1):L137-L147.

14. Clancy DM, Sullivan GP, Moran HBT, et al. Extracellular Neutrophil Proteases Are Efficient Regulators of IL-1, IL-33, and IL-36 Cytokine Activity but Poor Effectors of Microbial Killing. *Cell Rep*. 2018;22(11):2937-2950.

15. Lachowicz-Scroggins ME, Dunican EM, Charbit AR, et al. Extracellular DNA, Neutrophil Extracellular Traps, and Inflammasome Activation in Severe Asthma. *Am J Respir Crit Care Med*. 2019;199(9):1076-1085.

16. Manzenreiter R, Kienberger F, Marcos V, et al. Ultrastructural characterization of cystic fibrosis sputum using atomic force and scanning electron microscopy. *J Cyst Fibros*. 2012;11(2):84-92.

17. Whitsett JA. Airway Epithelial Differentiation and Mucociliary Clearance. *Ann Am Thorac Soc*. 2018;15(Suppl 3):S143-S148.

18. Montefort S, Baker J, Roche WR, Holgate ST. The distribution of adhesive mechanisms in the normal bronchial epithelium. *Eur Respir J*. 1993;6(9):1257-1263.

19. Nawijn MC, Hackett TL, Postma DS, van Oosterhout AJ, Heijink IH. E-cadherin: gatekeeper of airway mucosa and allergic sensitization. *Trends Immunol*. 2011;32(6):248-255.

20. Man Y, Hart VJ, Ring CJ, Sanjar S, West MR. Loss of epithelial integrity resulting from E-cadherin dysfunction predisposes airway epithelial cells to adenoviral infection. *Am J Respir Cell Mol Biol*. 2000;23(5):610-617.

21. Reboud E, Bouillot S, Patot S, Béganton B, Attrée I, Huber P. Pseudomonas aeruginosa ExlA and Serratia marcescens ShlA trigger cadherin

cleavage by promoting calcium influx and ADAM10 activation. *PLoS Pathog*. 2017;13(8):e1006579.

22. Cichy J, Potempa J, Travis J. Biosynthesis of alpha1-proteinase inhibitor by human lung-derived epithelial cells. *J Biol Chem*. 1997;272(13):8250-8255.

23. du Bois RM, Bernaudin JF, Paakko P, et al. Human neutrophils express the alpha 1-antitrypsin gene and produce alpha 1-antitrypsin. *Blood*. 1991;77(12):2724-2730.

24. Clemmensen SN, Jacobsen LC, Rørvig S, et al. Alpha-1-antitrypsin is produced by human neutrophil granulocytes and their precursors and liberated during granule exocytosis. *Eur J Haematol*. 2011;86(6):517-530.

25. McCarthy C, Reeves EP, McElvaney NG. The Role of Neutrophils in Alpha-1 Antitrypsin Deficiency. *Ann Am Thorac Soc*. 2016;13 Suppl 4:297.

26. Najmeh S, Cools-Lartigue J, Giannias B, Spicer J, Ferri LE. Simplified Human Neutrophil Extracellular Traps (NETs) Isolation and Handling. *Journal of Visualized Experiments*. 2015(98).

27. Haws C, Krouse ME, Xia Y, Gruenert DC, Wine JJ. CFTR channels in immortalized human airway cells. *Am J Physiol*. 1992;263(6 Pt 1):692.

28. Brewington JJ, Backstrom J, Feldman A, et al. Chronic β2AR stimulation limits CFTR activation in human airway epithelia. *JCI Insight*. 2018;3(4):e93029. doi: 10.1172/jci.insight.93029. eCollection 2018 Feb 22.

29. Fuchs HJ, Borowitz DS, Christiansen DH, et al. Effect of aerosolized recombinant human DNase on exacerbations of respiratory symptoms and on pulmonary function in patients with cystic fibrosis. The Pulmozyme Study Group. *N Engl J Med*. 1994;331(10):637-642.

30. Zaidman NA, O'Grady KE, Patil N, et al. Airway epithelial anion secretion and barrier function following exposure to fungal aeroallergens: role of oxidative stress. *Am J Physiol Cell Physiol*. 2017;313(1):C68-C79.

31. McGraw MD, Kim SY, White CW, Veress LA. Acute cytotoxicity and increased vascular endothelial growth factor after in vitro nitrogen mustard vapor exposure. *Ann N Y Acad Sci*. 2020;1479(1):223-233.

32. Marudamuthu AS, Bhandary YP, Fan L, et al. Caveolin-1-derived peptide limits development of pulmonary fibrosis. *Sci Transl Med*. 2019;11(522):eaat2848. doi: 10.1126/scitranslmed.aat2848.

33. Park CG, Lee SY, Kandala G, Lee SY, Choi Y. A novel gene product that couples TCR signaling to Fas(CD95) expression in activation-induced cell death. *Immunity*. 1996;4(6):583-591.

34. Zhang HY, Gharaee-Kermani M, Phan SH. Regulation of lung fibroblast alpha-smooth muscle actin expression, contractile phenotype, and apoptosis by IL-1beta. *J Immunol*. 1997;158(3):1392-1399.

35. Abbate A, Salloum FN, Van Tassell BW, et al. Alterations in the interleukin-1/interleukin-1 receptor antagonist balance modulate cardiac remodeling following myocardial infarction in the mouse. *PLoS One*. 2011;6(11):e27923.

36. Zhu K, Liang W, Ma Z, et al. Necroptosis promotes cell-autonomous activation of proinflammatory cytokine gene expression. *Cell Death Dis*. 2018;9(5):500-y.

37. Zou H, Yang R, Hao J, et al. Regulation of the Apaf-1/caspase-9 apoptosome by caspase-3 and XIAP. *J Biol Chem*. 2003;278(10):8091-8098.

38. Faust H, Mangalmurti NS. Collateral damage: necroptosis in the development of lung injury. *Am J Physiol Lung Cell Mol Physiol*. 2020;318(2):L215-L225.

39. Mertens AE, Roovers RC, Collard JG. Regulation of Tiam1-Rac signalling. *FEBS Lett*. 2003;546(1):11-16.

40. Salo S, Haakana H, Kontusaari S, Hujanen E, Kallunki T, Tryggvason K. Laminin-5 promotes adhesion and migration of epithelial cells: identification of a migration-related element in the gamma2 chain gene (LAMC2) with activity in transgenic mice. *Matrix Biol*. 1999;18(2):197-210.

41. Reinhold WC, Reimers MA, Lorenzi P, et al. Multifactorial regulation of E-cadherin expression: an integrative study. *Mol Cancer Ther*. 2010;9(1):1-16.

42. Matrisian LM. The matrix-degrading metalloproteinases. *Bioessays*. 1992;14(7):455-463.

43. Schlingmann B, Molina SA, Koval M. Claudins: Gatekeepers of lung epithelial function. *Semin Cell Dev Biol*. 2015;42:47-57.

44. Van Itallie C, Rahner C, Anderson JM. Regulated expression of claudin-4 decreases paracellular conductance through a selective decrease in sodium permeability. *J Clin Invest*. 2001;107(10):1319-1327.

45. Hou J, Renigunta A, Yang J, Waldegger S. Claudin-4 forms paracellular chloride channel in the

kidney and requires claudin-8 for tight junction localization. *Proc Natl Acad Sci U S A*. 2010;107(42):18010-18015.

46. Amasheh S, Fromm M, Günzel D. Claudins of intestine and nephron - a correlation of molecular tight junction structure and barrier function. *Acta Physiol (Oxf)*. 2011;201(1):133-140.

47. Morita K, Sasaki H, Fujimoto K, Furuse M, Tsukita S. Claudin-11/OSP-based tight junctions of myelin sheaths in brain and Sertoli cells in testis. *J Cell Biol*. 1999;145(3):579-588.

48. Urban CF, Ermert D, Schmid M, et al. Neutrophil extracellular traps contain calprotectin, a cytosolic protein complex involved in host defense against Candida albicans. *PLoS Pathog*. 2009;5(10):e1000639.

49. Knoell DL, Ralston DR, Coulter KR, Wewers MD. Alpha 1-antitrypsin and protease complexation is induced by lipopolysaccharide, interleukin-1beta, and tumor necrosis factor-alpha in monocytes. *Am J Respir Crit Care Med*. 1998;157(1):246-255.

50. Lefrançais E, Mallavia B, Zhuo H, Calfee CS, Looney MR. Maladaptive role of neutrophil extracellular traps in pathogen-induced lung injury. *JCI Insight*. 2018;3(3):e98178. doi: 10.1172/jci.insight.98178. eCollection 2018 Feb 8.

51. Narasaraju T, Yang E, Samy RP, et al. Excessive neutrophils and neutrophil extracellular traps contribute to acute lung injury of influenza pneumonitis. *Am J Pathol*. 2011;179(1):199-210.

52. Xiao C, Puddicombe SM, Field S, et al. Defective epithelial barrier function in asthma. *J Allergy Clin Immunol*. 2011;128(3):549-12.

53. Martínez-Alemán SR, Campos-García L, Palma-Nicolas JP, Hernández-Bello R, González GM, Sánchez-González A. Understanding the Entanglement: Neutrophil Extracellular Traps (NETs) in Cystic Fibrosis. *Front Cell Infect Microbiol*. 2017;7:104.

54. Hudock KM, Imbrogno M, Collins MS, Brewington JJ, Kramer EL, O'Shaugnessy RA, Ostmann AJ, Clancy JP. Neutrophil Extracellular Trap Burden in CF and Disease Control BAL. [published online ahead of print May]. *American Journal of Respiratory and Critical Care Medicine*.

55. Goto Y, Uchida Y, Nomura A, et al. Dislocation of E-cadherin in the airway epithelium during an antigen-induced asthmatic response. *Am J Respir Cell Mol Biol*. 2000;23(6):712-718.

56. Wray C, Mao Y, Pan J, Chandrasena A, Piasta F, Frank JA. Claudin-4 augments alveolar epithelial barrier function and is induced in acute lung injury. *Am J Physiol Lung Cell Mol Physiol*. 2009;297(2):219.

57. Molenda N, Urbanova K, Weiser N, Kusche-Vihrog K, Günzel D, Schillers H. Paracellular transport through healthy and cystic fibrosis bronchial epithelial cell lines--do we have a proper model? *PLoS One*. 2014;9(6):e100621.

58. Molina SA, Moriarty HK, Infield DT, et al. Insulin signaling via the PI3-kinase/Akt pathway regulates airway glucose uptake and barrier function in a CFTR-dependent manner. *Am J Physiol Lung Cell Mol Physiol*. 2017;312(5):L688-L702.

59. Abdul-Hafez A, Mohamed T, Uhal BD. Activation of mas restores hyperoxia-induced loss of lung epithelial barrier function through inhibition of apoptosis. *J Lung Pulm Respir Res*. 2019;6(3):58-62.

60. White SR. Apoptosis and the airway epithelium. *J Allergy (Cairo)*. 2011;2011:948406.

61. Saffarzadeh M, Juenemann C, Queisser MA, et al. Neutrophil extracellular traps directly induce epithelial and endothelial cell death: a predominant role of histones. *PLoS One*. 2012;7(2):e32366.

62. Suzuki T, Moraes TJ, Vachon E, et al. Proteinase-activated receptor-1 mediates elastase-induced apoptosis of human lung epithelial cells. *Am J Respir Cell Mol Biol*. 2005;33(3):231-247.

63. Shen J, Vakifahmetoglu H, Stridh H, Zhivotovsky B, Wiman KG. PRIMA-1(MET) induces mitochondrial apoptosis through activation of caspase-2. *Oncogene*. 2017;36(25):3650.

64. Tian X, Liu Z, Niu B, et al. E-cadherin/β-catenin complex and the epithelial barrier. *J Biomed Biotechnol*. 2011;2011:567305.

65. Boxio R, Wartelle J, Nawrocki-Raby B, et al. Neutrophil elastase cleaves epithelial cadherin in acutely injured lung epithelium. *Respir Res*. 2016;17(1):129-x.

66. Evans SM, Blyth DI, Wong T, Sanjar S, West MR. Decreased distribution of lung epithelial junction proteins after intratracheal antigen or lipopolysaccharide challenge: correlation with neutrophil influx and levels of BALF sE-cadherin. *Am J Respir Cell Mol Biol*. 2002;27(4):446-454.

67. Chillappagari S, Preuss J, Licht S, et al. Altered protease and antiprotease balance during a COPD exacerbation contributes to mucus obstruction. *Respir Res*. 2015;16(1):85-x.

68. Fazleen A, Wilkinson T. The emerging role of proteases in α(1)-antitrypsin deficiency and

beyond. *ERJ Open Res*. 2021;7(4):00494-2021. eCollection 2021 Oct.

69. Khan TZ, Wagener JS, Bost T, Martinez J, Accurso FJ, Riches DW. Early pulmonary inflammation in infants with cystic fibrosis. *Am J Respir Crit Care Med*. 1995;151(4):1075-1082.

70. Sly PD, Gangell CL, Chen L, et al. Risk factors for bronchiectasis in children with cystic fibrosis. *N Engl J Med*. 2013;368(21):1963-1970.

71. Crisford H, Sapey E, Rogers GB, et al. Neutrophils in asthma: the good, the bad and the bacteria. *Thorax*. 2021;76(8):835-844.

72. Ray A, Kolls JK. Neutrophilic Inflammation in Asthma and Association with Disease Severity. *Trends Immunol*. 2017;38(12):942-954.

73. Frenzel E, Korenbaum E, Hegermann J, et al. Does augmentation with alpha1-antitrypsin affect neutrophil extracellular traps formation? *Int J Biol Sci*. 2012;8(7):1023-1025.

74. Huntington JA, Read RJ, Carrell RW. Structure of a serpin-protease complex shows inhibition by deformation. *Nature*. 2000;407(6806):923-926.

75. Brantly M. Alpha1-antitrypsin: not just an antiprotease: extending the half-life of a natural anti-inflammatory molecule by conjugation with polyethylene glycol. *Am J Respir Cell Mol Biol*. 2002;27(6):652-654.

76. Janciauskiene S, Wrenger S, Immenschuh S, et al. The Multifaceted Effects of Alpha1-Antitrypsin on Neutrophil Functions. *Front Pharmacol*. 2018;9:341.

77. Hoffmann JH, Schaekel K, Gaiser MR, Enk AH, Hadaschik EN. Interindividual variation of NETosis in healthy donors: introduction and application of a refined method for extracellular trap quantification. *Exp Dermatol*. 2016;25(11):895-900.

78. Fulcher ML, Gabriel S, Burns KA, Yankaskas JR, Randell SH. Well-differentiated human airway epithelial cell cultures. *Methods Mol Med*. 2005;107:183-206.

79. Kramer EL, Madala SK, Hudock KM, Davidson C, Clancy JP. Subacute TGFβ Exposure Drives Airway Hyperresponsiveness in Cystic Fibrosis Mice through the PI3K Pathway. *Am J Respir Cell Mol Biol*. 2020;62(5):657-667.

80. Krämer A, Green J, Pollard J,Jr, Tugendreich S. Causal analysis approaches in Ingenuity Pathway Analysis. *Bioinformatics*. 2014;30(4):523-530.

81. Chen J, Bardes EE, Aronow BJ, Jegga AG. ToppGene Suite for gene list enrichment analysis and candidate gene prioritization. *Nucleic Acids Res*. 2009;37(Web Server issue):305.

82. Chen X, Shank S, Davis PB, Ziady AG. Nucleolin-mediated cellular trafficking of DNA nanoparticle is lipid raft and microtubule dependent and can be modulated by glucocorticoid. *Mol Ther*. 2011;19(1):93-102.

83. Ziady AG, Kinter M. Protein sequencing with tandem mass spectrometry. *Methods Mol Biol*. 2009;544:325-341.

84. Chen J, Kinter M, Shank S, Cotton C, Kelley TJ, Ziady AG. Dysfunction of Nrf-2 in CF epithelia leads to excess intracellular H2O2 and inflammatory cytokine production. *PLoS One*. 2008;3(10):e3367.

85. Korkmaz B, Attucci S, Juliano MA, et al. Measuring elastase, proteinase 3 and cathepsin G activities at the surface of human neutrophils with fluorescence resonance energy transfer substrates. *Nat Protoc*. 2008;3(6):991-1000.